Contract No. NAS5-30310

SBIR- 08.04-2701
release date 5/09/92 ✓

LARGE AREA NUCLEAR PARTICLE DETECTORS USING ET MATERIALS - PHASE II

Charles Y. Wrigley
George M. Storti
Lee Walter
Scott Mathews

Quantex Corporation
2 Research Court
Rockville, Maryland 2085^

May 1990
Final Report

Prepared for

Goddard Space Flight Center
Greenbelt, Maryland 20771

TECHNICAL REPORT STANDARD TITLE PAGE

1. Report No.	2. Government Accession No.	3. Recipient's Catalog No.

4. Title and Subtitle	5. Report Date
Large Area Nuclear Particle Detectors Using ET Materials - Phase II	May 1990
	6. Performing Organization Code
7. Author(s) C. Wrigley, G. Storti, L. Walter and S. Mathews	8. Performing Organization Report No. LAPD-FINAL
9. Performing Organization Name and Address Quantex Corporation 2 Research Court Rockville, Maryland 20850	10. Work Unit No.
	11. Contract or Grant No. NAS5-30310
	13. Type of Report and Period Covered Final 5/9/88 - 5/9/90
12. Sponsoring Agency Name and Address NASA/Goddard Space Flight Center Greenbelt, Maryland 20771 Jonathon Ormes	14. Sponsoring Agency Code

15. Supplementary Notes

16. Abstract

This report presents work done under a Phase II SBIR contract for demonstrating large area detector planes utilizing Quantex electron trapping (ET™) materials as a film medium for storing high-energy nuclide impingement information. The detector planes utilize energy dissipated by passage of the high-energy nuclides to produce localized populations of electrons stored in traps. Readout of the localized trapped electron populations is effected by scanning the ET plane with near-infrared, which frees the trapped electrons and results in optical emission at visible wavelengths. The effort involved both optimizing fabrication technology for the detector planes and developing a readout system capable of high spatial resolution for displaying the recorded nuclide passage tracks.

17. Key Words (Selected by Author(s))	18. Distribution Statement
Particle Detectors, ET Storage, Cosmic Rays, Electron Trapping	See SBIR Rights Notice (June 1987)

19. Security Classif. (of this report)	20. Security Classif. (of this page)	21. No. of Pages	22. Price*
Unclassified	Unclassified	32	

PREFACE

Objective

This final report concerns a Phase II SBIR contract with the objective of demonstrating the application of Quantex electron trapping (ET™) materials to the recording of high-energy atomic nuclei passage through a plane sheet and subsequent readout of the locations of impingement. The Phase I SBIR contract effort showed that such a recording technique was feasible, and this Phase II work has demonstrated its objective of reduction to hardware prototypes. The driving interest on the part of NASA/GSFC has been to locate such relativistic-velocity nuclei "tracks" to an accuracy of 20 micrometers or better, so that the various cosmic ray species could be identified.

The Quantex ET materials store information on dissipated energy produced by transiting high energy nuclei by trapping excited electrons (or excitons) in deep (about 1 eV) trap states. These electron traps are so deep that usual thermal agitation cannot dislodge more than a tiny fraction of a stored electron population over long storage times, but the trapped electrons can be instantly freed on demand by near-infrared and produce visible light emission as they quickly drop in energy at rare-earth luminescent centers. The result is a recording screen of arbitrarily large dimensions that can produce visible-light readout by scanning with a near-infrared laser beam, i.e., an all-solid-state equivalent of photographic film, but requiring no wet chemistry.

Scope of Work

Quantex initially started this Phase II work with the aim of applying either thin vapor-deposited ET films or thin powder ET layers to rigid substrates. Later in the project it became quite obvious that it would be better for GSFC application purposes to generate films on lightweight thin sheets of low-Z organic polymers. This produced a shift in direction of the R & D work, to generate such films. The Quantex ET materials are polycrystalline alkaline-earth sulfides which require high temperatures (around 1000°C) of fabrication. Either vapor-deposited thin films or powder films can be formed in-situ on refractory substrates, but this was out of the question for polymer sheets. Consequently, Quantex refined its process techniques for making fine ET powders that are electronically and optically suitable for subsequent device fabrication at polymer-compatible temperatures. This was successfully accomplished and storage screens were indeed made on thin polyesters and polyimides. Films of 75 micrometer thickness were generated to reach the GSFC goal of resolving transit locations to <20 micrometers upon readout.

In order to read the stored location information from the ET films, Quantex constructed a prototype readout scanning system during Phase II. This scanner utilizes a diode-pumped all-solid-state YAG:Nd laser, a precision x-y stepping table, uncomplicated optics, and an electronic digitizing image processor working with a microcomputer for video display.

Conclusions

This SBIR Phase II effort has defined the requirements for a detector plane that will record the passage of a spectrum of cosmic ray particles, and such planes have been fabricated. This work has involved the development of techniques for producing high efficiency electron trapping powders as well as for fabricating detector planes.

Although no substantial commercial use for a cosmic ray detector is foreseen, these same detector planes are likely to have a myriad of uses in the commercial marketplace, since they are sensitive to all types of ionizing radiation. The extended dynamic range of this system vs. photographic film would offer definite advantages in such areas and the direct data capture would facilitate image analysis. Among the readily identifiable uses are radiation beam pattern profiling, autoradiography (e.g., isotope tagged biological materials), industrial radiography, crystallography, and medical radiography.

Quantex is pursuing a number of these applications, both with internal funds and with the support of commercial partners. Consequently, the work performed in this Phase II effort has been very successful with regards to its particular objectives and to the overall objectives of the SBIR program.

Summary of Recommendations

For the various likely commercial applications or larger volume applications to NASA projects, it would be advisable to complete engineering implementation of powder manufacturing systems such as inert-gas jet milling and cyclone particle size separation for production quantities. Such equipment was beyond the financial scope of the Phase II work, but is readily available.

It would be highly worthwhile to proceed on to NASA tests with accelerator-produced high-energy nuclide mapping and then to balloon-flight sampling of cosmic-ray relativistic nuclide recording trials. This would provide a final demonstration of the capabilities of the ET detector plane system and data for subsequent NASA application in orbital experiments.

Table of Contents

List of Illustrations

List of Tables

List of Tables

List of Abbreviations and Symbols

A	Atomic Weight
C	Speed of Light
E_q	Semiconductor forbidden energy gap
ET	Electron Trapping
IRSL	Infrared Stimulated Luminescence
m_e	Electron Rest Mass
SNR	Signal to Noise Ratio
V	Particle Velocity
Z	Atomic Number
γ	Lorentz Factor

OBJECTIVES:

The proposed objectives for this Phase II SBIR contract effort were the following:

1) The first Technical Objective was the optimization of specific ET materials and device structures for various energetic particulate radiation species. This required completing the materials and device technology research for thick-film and thin-film embodiments suitable for detectors of various species.

2) The second Technical Objective was to design, build and exercise prototype readout instrumentation capable of high-resolution serial scanning, or parallel area-wide, image capture of large-area ET detector planes after high-energy particulate species exposures to distributed events over at least 100 cm^2 areas per readout.

3) The third Technical Objective was to show that the materials and device structures generated to satisfy Objective 1, when employed in combination with the prototype readout instrumentation generated to satisfy Objective 2, provide stored event information in sufficient resolution and magnitudes to be a very useful addition to the previously available range of detectors.

4) The fourth Technical Objective was to generate sufficiently detailed documentation of the Phase II research as to provide direct transition to Phase III engineering implementation of ET detector planes and associated readout instrumentation in an initial product manufacturing environment.

It was expected that attainment of these Technical Objectives would generate the requisite confidence for Phase III success of the ET energetic particle detectors in private-sector development and manufacturing.

PHASE II STATEMENT OF WORK:

The principal objective of the proposed Phase II effort was to demonstrate operating large area nuclear particle detectors that are in a state of readiness for Phase III transition. In order to accomplish this, we proposed the following tasks:

Task 1: Materials and Device Research

The contractor shall parametrically investigate the ET material formulations, preparations and configurations for generating large-area detector devices. Detectors of species sensitivities and large-area geometries mutually agreeable with the cognizant NASA/ Goddard Space Flight Center Technical Officer shall be fabricated in quantities sufficient for performance of Tasks 3 and 4.

Task 2: Prototype Readout System

The contractor shall design, assemble and check out operation of a prototype near-infrared stimulated luminescence prototype readout system. The system shall be compatible with the detector geometries of Task 1. It shall have a light-tight enclosure for the detector(s) employed, internal erasure means, an activator mechanism for test radionuclide sources and two-dimensional information display, at a microcomputer level of complexity. Spatial resolution shall be as proposed.

Task 3: System Evaluation

The contractor shall utilize the prototype readout system of Task 2 to evaluate ET detectors generated in Task 1. The detectors shall be exercised for the energetic particle species agreed with the Technical Officer in Task 1, using appropriate broad-area sources of mutually agreeable activity levels.

Task 4: Preparations for Phase III

The contractor shall prepare documentation of the efforts conducted under Tasks 1, 2 and 3 in a form suitable for use as baseline process specifications, process control tradeoffs, design guidelines, performance criteria, projected manufacturing costs and manufacturing equipment projections.

Task 5: Reporting

The contractor shall prepare quarterly progress reports and a final report in the manner specified by NASA/GSFC.

THE WORK PERFORMED:

Introduction

An important guide to the work reported herein has been the phenomenological model for the physical processes occurring in the ET material (SrS:Ce,Sm). This model has been considerably refined over the course of the Phase II contract, and has assisted in directing efforts on the materials, the devices and the read-out system. Our current understanding of the physical processes and their impact on the potential for detecting high energy cosmic rays is presented below.

High energy nuclear particles will undergo energy losses when transiting through a media. The interaction of these high energy particles with the nuclei and electrons of the media result in the generation of electron-hole pairs. In semiconductors such as the ET materials, one electron-hole pair is generated for each 3 E_q (where E_q is the band gap energy) increment of energy lost by the impinging particle. Given that the energy gap of SrS is 4.3 eV[1], approximately 13 eV is required to produce an electron-hole pair. The electron-hole pairs quickly form indirect-bandgap excitons that will not easily recombine because the transition is quantum mechanically unfavorable. However, the introduction of rare-earth atoms ("impurities") into the host lattice brings in a recombination path that can be optically radiative[1]. Most likely, the indirect-bandgap excitons become trapped at the impurity locations, thereby becoming bound excitons. The forbidden aspect of the transition in the host lattice is removed and the electrons and holes recombine and transfer energy to ground-state electrons of the impurity.

If there is a single impurity such as Ce^{3+}, the ground state electron makes the transition to excited states and returns to the ground state with the emission of a characteristic luminescence. If there are two impurities (e.g., Ce^{3+}, Sm^{3+}), there is competition between recombination at Ce^{3+} or Sm^{3+}. However, if electron trapping is to occur, the primary recombination path must be through the cerium atoms in the lattice. The electron in the Ce^{3+} excited states resulting from the recombination of the bound excitons can transfer over to Sm^{3+} atoms (charge exchange), transfer to some other defect site, or return to the Ce^{3+} ground state with the emission of the characteristic luminescence. The charge exchange with samarium is very highly likely if the samarium atoms are located within tunneling distances (a few lattice spacings) of the cerium atoms.

Once excited electrons have transferred to samarium atoms, they relax to the ground state of what is then Sm^{2+}. Transitions out of this state appear to be forbidden except by rising to higher excited states of Sm^{2+}. At room temperature, there is insufficient thermal energy to excite the Sm^{2+} ground-state electron to higher excited states, but optical radiation having wavelengths between 800 and 1500 nm <u>can</u> cause the elevation to the excited levels, from which an electron can tunnel over to nearby cerium excited levels. The electron will fall to the lower-energy levels of the cerium excited states and can then de-energize to the cerium ground state, emitting characteristic Ce^{3+} photons. This latter process is called infrared-stimulated luminescence, or IRSL. The resulting spectral response to near-infrared and the spectral emission are as shown in Figure 1.

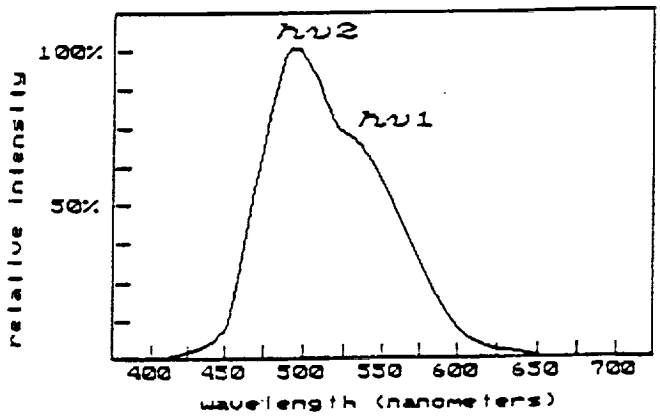

a. Luminescence spectrum.

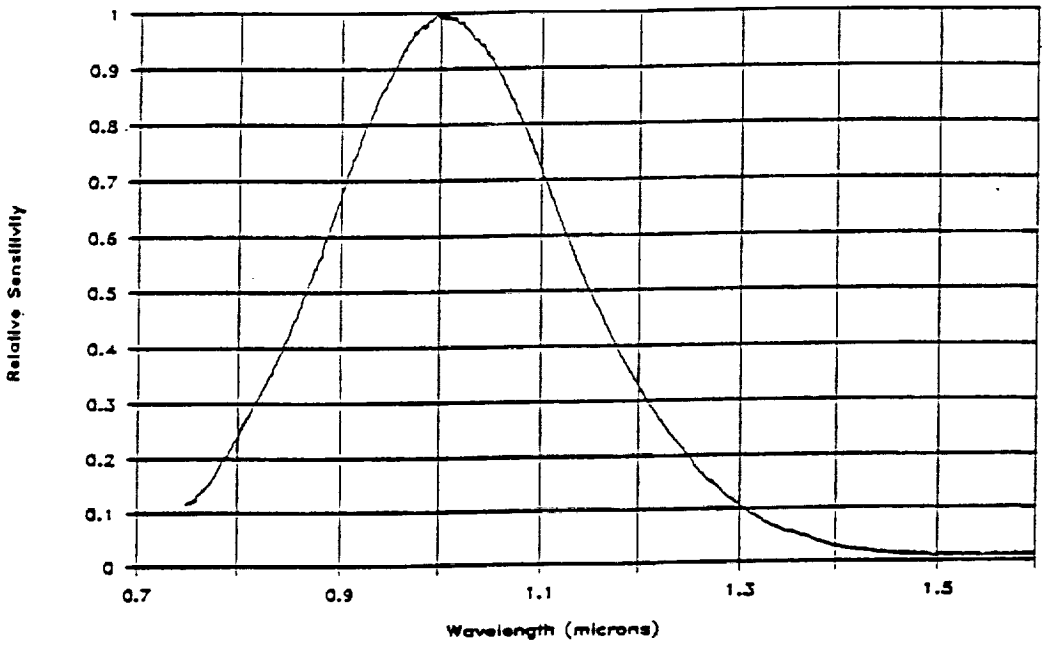

b. Infrared sensitivity spectrum.

Figure 1. IR sensitivity and visible emission spectra for SrS:Ce,Sm.

If the indirect-bandgap exciton becomes bound to Sm^{3+} and de-excites there, only the sharp-line luminescence characteristic of Sm^{3+} would be expected, since no electron exchange with cerium will occur, because neither Ce^{2+} nor Sm^{4+} are possible electronic configurations for the dopants.

Energy transfer from an exciton to a valence-band electron could result in Sm^{2+} (i.e., converting Sm^{3+} to Sm^{2+}), but any luminescence that would be produced would either be that from Ce^{3+} (due to charge transfer from a Sm^{2+} excited state to Ce^{4+}) or from Sm^{2+}, which would have a peak emission in the infrared. If cerium emission is to occur, it is necessary that a cerium atom in its 4+ state be in proximity to the Sm^{2+}. Given that cerium is normally in a 3+ state prior to excitation by UV light or energetic particles, and that a Ce^{4+} configuration could only be produced by charge transfer between Ce^{3+} and another defect, it appears that the transition from the Sm^{2+} to Ce^{4+} is not very probable. If the exciton energy transfer results in a Sm^{2+}, it is also not very probable that Ce^{3+} emission would be observed when the Sm^{2+} is excited with infrared light.

It is possible that a non-radiative process is associated with the energy transfer mentioned above, but there are presently no data to confirm or deny that process.

In summary, the most likely model for describing the physical processes occurring in these ET materials is as described above. A number of implications flow from this model concerning doping concentrations. Clearly, because tunnelling processes are involved, the distance between cerium and samarium atoms on average needs to be small if trapping is to be maximized. However, there is an optimum doping concentration beyond which the light output decreases. The reason for this is not clear, but the formation of local clusters of a new phase is a possibility - for example, the dopant(s) may form a new phase with the sulfur.

Maximizing the trapping center density is also important with respect to the interaction volume the high energy particles have with the phosphor layer. At very high energies, the interaction volume is greatest at initial entry into any material. In particular, so-called delta rays (high energy electrons) are produced in the interaction between the nucleons and electrons of the phosphor. Much of the energy loss occurs via the production of the delta rays. These delta rays in turn lose energy by generating electron-hole pairs throughout a volume that is considerably larger than that associated with the path of the heavy particle itself. This is advantageous for maximizing the trapped electron population.

With these considerations in mind, a major focus of the Phase II efforts has been to enhance the performance characteristics of the ET material and to maintain those characteristics in the detector planes fabricated from the materials. Several detector plane fabrication methods were investigated, and in the latter stages of the contract, efforts were directed towards producing planes of ET material on thin polymer substrates. Detector planes were evaluated on either one or both of two scanning systems. Further, the scanning systems themselves were evaluated so that recommendations for an appropriate system for the applications addressed in the contract could be made. A detailed report of this work is presented below.

Task 1: Materials and Device Research

Materials Research Efforts

ET material performance was an important factor in the success of this effort. Consequently, a considerable portion of the Phase II effort was directed toward its optimization. During the contract term, a better understanding of the physical mechanisms operating within the ET materials was gained, and this understanding indicated that increased amounts of the cerium and samarium dopants had the potential to increase the trapping capacity and the infrared readout efficiency. In addition, reduction of unintentional impurities and lattice defects was also likely to improve performance, since the effects of possible alternate trapping sites and recombination paths would be minimized. To this end, dopants were introduced in their halide and sulfide forms, and the flux that assists in dopant incorporation was supplemented by a sulfur-rich constituent (Li_2S). The additional sulfur present was expected to reduce sulfur vacancy formation during high temperature treatments, halides were more temperature compatible, etc.

During the contract work the patented Quantex "Q-16" SrS:Ce,Sm ET Material (U.S. patent no. 4,822,520, called Standard Material hereafter) that was improved consisted of three major components; the alkaline earth host (strontium sulfide), rare earth dopants (cerium and samarium) in oxide and sulfide forms, and alkalai halide (lithium fluoride) and alkaline sulfate (barium sulfate) flux additives. The ET bulk and powder materials were worked on in parallel development efforts. The bulk material was permuted to improve its ET properties via simplifying the material chemistry, coupled with material variations. The powder processing of the material was developed to retain the bulk ET properties via developments in three components that establish the powder process; grinding, chemical etching and thermal reactivation. Both of these efforts were also aided by parallel work funded internally and by commercial funding aimed at other applications of ET materials.

The main objectives in the efforts in both the bulk material and powder process development were improving the IR Stimulated Luminescence (IRSL) output and the electron trap retention* properties of the material. The quality of and improvement in the ET material was evaluated by monitoring the IRSL output (in microW/cm^2 under 1.06 micron infrared input of 2mW/cm^2). The IRSL output was obtained by stimulating the ET material with 1.06 micron light after U.V. charging for 30 seconds. The trapped electron retention properties were obtained via initial U.V. charging and delaying the application of IR stimulation for evaluating the luminescence output over a range of times.

* "Retention" refers to the maintenence of a trapped electron population over extended time, as measured by the integral of visible-wavelength photons produced by infrared stimulation. The decay function follows an inverse power function of elapsed time, e.g., (const.)$t^{-0.2}$.

ET Ingot Material Optimization

The bulk ET material was optimized in an iterative process consisting of simplifying the material chemistry, varying the content of the chemical components and varying the form of the components. The initial step in the material development (Matrl 1) was to simplify the material chemistry and provide chemical compatibility for all material components. This was accomplished by replacing barium sulfate in the Standard Material (Matrl 0) with lithium sulfide. The addition of the lithium sulfide was to enhance chemical compatibility of the material components via common ion effects. Additionally, lithium sulfide is also a lower melting point compound (i.e. 900-950°C) than barium sulfate (i.e., 1580-1600°C) with comparable thermodynamic properties to lithium fluoride. This variation provided more favorable thermodynamic conditions for crystallizing the material when processed at lower temperatures.

The optimum concentrations of both the dopants and the flux additives were then re-established. This variation (Matrl 2) established the optimum concentration of samarium oxide and cerium sulfide to be 23 ppm and 217 ppm, respectively. The optimum concentrations of lithium fluoride and lithium sulfide were similarly established to be 28.8 and 1.8 mole %, respectively. To further simplify the material chemistry, cerium sulfide and samarium oxide dopants were changed to cerium chloride and samarium chloride. This material variation (Matrl 3) further enhanced the chemical compatibility of the dopants with the remaining components of the material and simplified the material chemistry further through common ion effects. The chloride form of the dopants are low temperature compounds (i.e. 900-950°C) comparable to flux components with similar thermodynamic properties and therefore also provided more favorable thermodynamic conditions for crystallizing the material when heated. The optimum concentration of the chloride dopants in this material variation (Matrl 4) was found to be 45 ppm cerium chloride and 45 ppm samarium chloride. The optimum flux component concentration remained the same as in Matrl 3. To further enhance environmental stability, chemical compatibility and improve thermodynamic conditions for crystallizing the phosphor material, lithium carbonate replaced lithium sulfide in the flux component of the material (Matrl 5). Lithium carbonate has a much lower melting point (i.e. 750°C) than lithium sulfide and similarly provides favorable thermodynamic conditions for crystallizing the material. Lithium carbonate also posesses a favorable chemical property, in that it decomposes to the oxide form, liberating carbon dioxide during the heating process and provides an environment-stable oxide that is incorporated into the ET material, with a resulting increase in the environmental stability of the resulting ET material.

Results of ET Material Variations

The results of the ET material permutations are presented in Figure 2 and Figure 3. The IRSL output improvements of the ET material as a function of the material variations, Matrl 0 through Matrl 5, are presented in Figure 2. As can be seen in Figure 2, an increase in IRSL output resulted for each material variation going from Matrl 0 to Matrl 5. The material optimization work has resulted in an increase of a factor of 3 in the IRSL output of ET Matrl 5 as compared to the Quantex Standard Material (Matrl 0). In Figure 3, the improvements in trap retention properties of the bulk material are shown as a function of the material variations. Similarly, the permutation work resulted in a substantial increase in the trap retention properties of Matrl 5 as compared to the initial version (Matrl 0).

The material optimization results showed substantial improvement in the IRSL output and a similar substantial improvement in the ET retention properties of the material for each iterative cycle in which the material chemistry of the phosphor was simplified and followed with subsequent compositional variations.

Powder Process Optimization

The ET powder process optimization effort focused primarily on refining our powder process so that bulk ET material is reduced to a powder material which retains the storage sensitivity and storage retention properties of the bulk material. The bulk crystalline material is generated in the form of an ingot. As the ingot is processed into a powder, mechanical damage results on the surface and within the ET particles. As the particle size of the powder decreases, more mechanical damage per unit volume results. As a consequence of the mechanical damage, both the IRSL output and the storage retention properties of the ET powder material are adversely affected. The major objectives of the process were to minimize mechanical damage in processing the bulk ingot into a powder and to repair the mechanical damage remaining. Three major operations constituted the powder process; the grinding of the bulk material ingot into a powder, chemical etching of the powder to remove or passivate any surface damage to the powder particles and the thermal reactivation of the etched powder to passivate any remaining surface and internal mechanical damage of the powder particles. The ET powders were generated in three different particle size distributions; 20-38 microns, 38-53 microns, and 53-106 microns.

To minimize initial mechanical damage in grinding the ingot, three methods being employed at Quantex for generating ET powder were evaluated. Ingots were powdered by: agate pulverizing (Method 1), hydraulic crushing (Method 2), and centrifugal ball milling (Method 3). The powders generated by each method were then sieved and the three particle size distributions collected. The powdering methods were also evaluated as a function of particle size and material variations (Matrl 0 through Matrl 5) defined above. Powdering via Method 3 was found to be the most effective in minimizing initial mechanical damage for all material variations and particle size distributions.

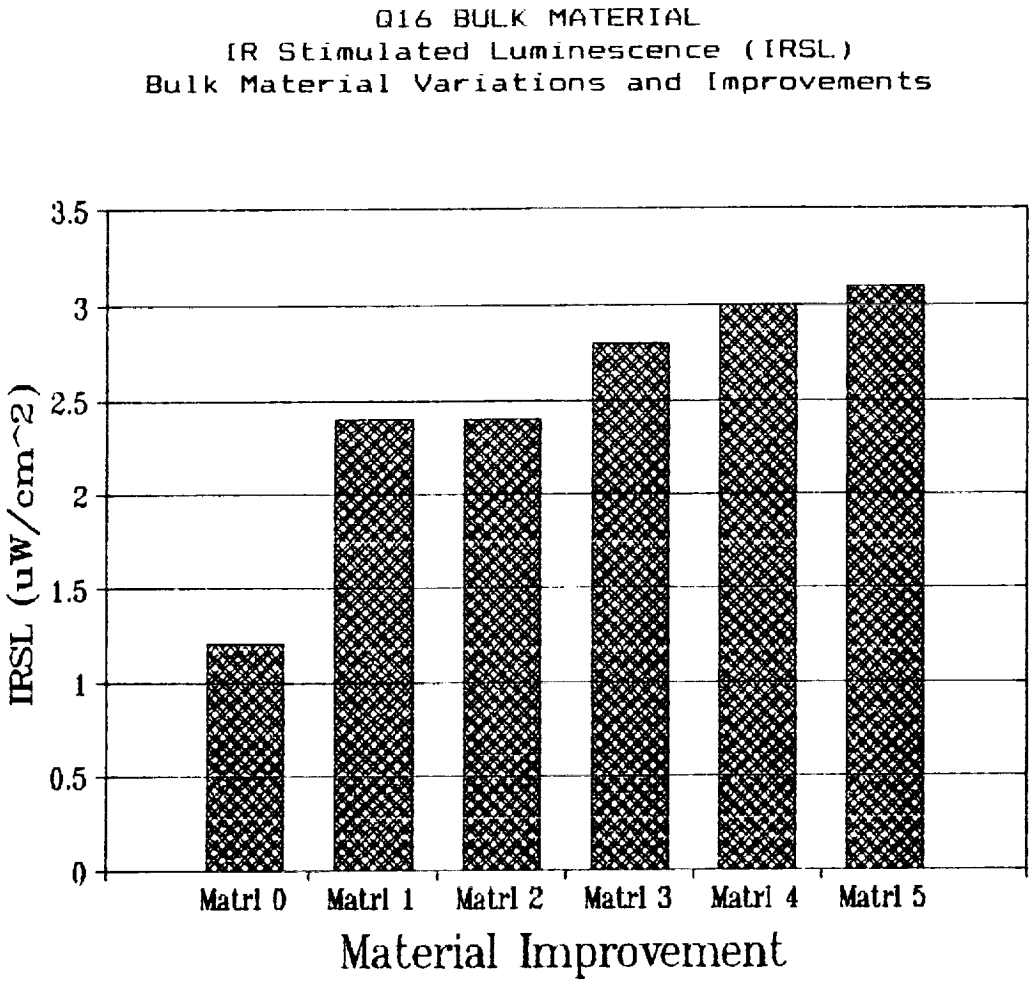

LEGEND
Material Improvement

Matrl 0	--	Standard Q16 Bulk Material.
Matrl 1	--	Material Chemistry Simplified. Alkalai Sulfide Flux Introduced.
Matrl 2	--	Dopant Concentration Change.
Matrl 3	--	Chloride Form of Dopant Introduced.
Matrl 4	--	Chloride Dopant Concentration Change.
Matrl 5	--	Alkalai Carbonate Flux Introduced.

Figure 2. IRSL Output for Q16 Bulk Material Variations and Improvements.

Q16 BULK MATERIAL
% RETENTION
1 Hour, U.V. Charged

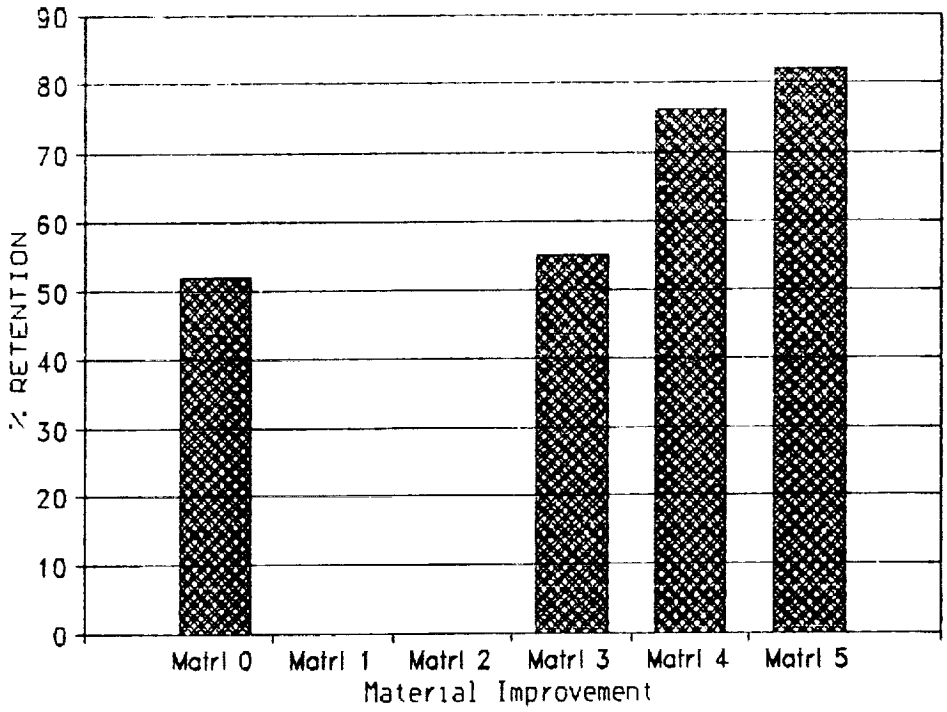

LEGEND
Material Improvement

Matrl 0	--	Standard Q16 Bulk Material.
Matrl 1	--	Material Chemistry Simplified. Alkalai Sulfide Flux Introduced.
Matrl 2	--	Dopant Concentration Change.
Matrl 3	--	Chloride Form of Dopant Introduced.
Matrl 4	--	Chloride Dopant Concentration Change.
Matrl 5	--	Alkalai Carbonate Flux Introduced.

Figure 3. Retention for Q-16 Bulk Material Corrections and Improvements.

Chemical etchants were used to evaluate the most effective method to passivate the surface of the powder particles. Various acidic and basic solutions were initially evaluated at room temperature and elevated temperatures up to 150°C for various time periods. ET powder generated via Methods 1 through 3 were then treated with the chemical etchants, filtered, dried and the IRSL output measured. The chemically etched powders were also evaluated as a function of particle size and material variations. Ammonia and ammonia-based etchants were found to be the most effective. To further repair any remaining mechanical damage in the powders, the powders were then thermally reactivated in a nitrogen environment at elevated temperatures (i.e. 550-600°C) for a time period of 30-60 minutes. Both pre-etched and etched powders were evaluated as a function of particle size and material variations. The most effective thermal reactivation temperature for all material variations and particle size distributions was found to be at 600°C for 30 minutes.

Powder Process Optimization Results

The results of the Q-16 ET powder process refinement effort are presented in Figures 4 through 8. Figures 4 through 8 present the results of each component of the process and the overall process as a whole.

The evaluation of the grinding method to minimize initial mechanical damage is presented in Figure 4 for Matrl 5. The IRSL output of the powder for grinding Method 1, Method 2 and Method 3 is presented for 20-38 micron and 38-53 micron size particle distributions. The IRSL output of the powder was enhanced by a factor of 3 as the grinding process was varied from Method 1 to Method 3. For the three grinding methods evaluated, the most effective method of powdering the ingot and minimizing initial mechanical damage in the powder was centrifugal ball milling.

The results of chemical etching using an ammonia etchant on the powder to improve the IRSL output are shown in Figure 5. In Figure 5, comparison of the IRSL output enhancement (i.e. IRSL(etched)/cRSL(non-etched)) for Matrl 0 and Matrl 4 for 20-38 micron and 53-106 micron particle distributions is shown. The IRSL output for Matrl 0 was enhanced by a factor of 1.3 for both particle size distributions. The IRSL output for Matrl 4 was enhanced by a factor of 5.5 for the 20-38 micron particle distribution and enhanced by a factor of 2.2 for the 53-106 micron particle size distribution. The variation in IRSL enhancement between the Standard Material (Matrl 0) and Matrl 4 indicates that the chemical etching is a function of the material composition and that ammonia was a more effective etchant when an alkalai sulfide and chloride dopants were employed. The variation in IRSL enhancement in Matrl 4 for the two particle size distributions indicates that more mechanical damage occurs for smaller particle size, but that an improvement in IRSL output results on chemical etching for smaller powder particle sizes.

The results of thermal reactivation of the non-etched ET powder to further improve the IRSL output are shown in Figure 6. In Figure 6, the IRSL output of Matrl 5 as a function of the thermal reactivation temperature for a 38-53 micron particle size distribution is presented with the initial non-etched powder denoted as "25°C". As the thermal reactivation

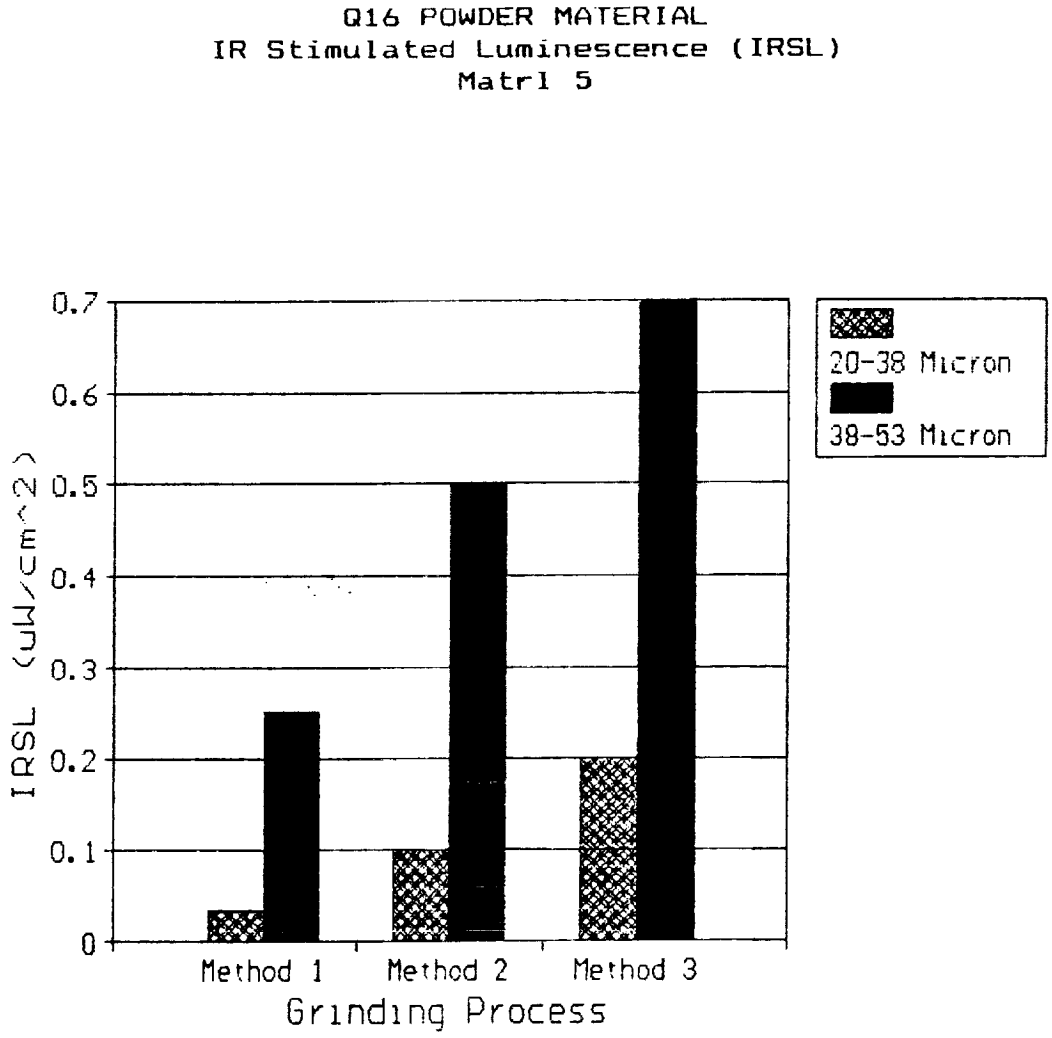

Figure 4. Powder IRSL Output for 3 Grinding Methods.

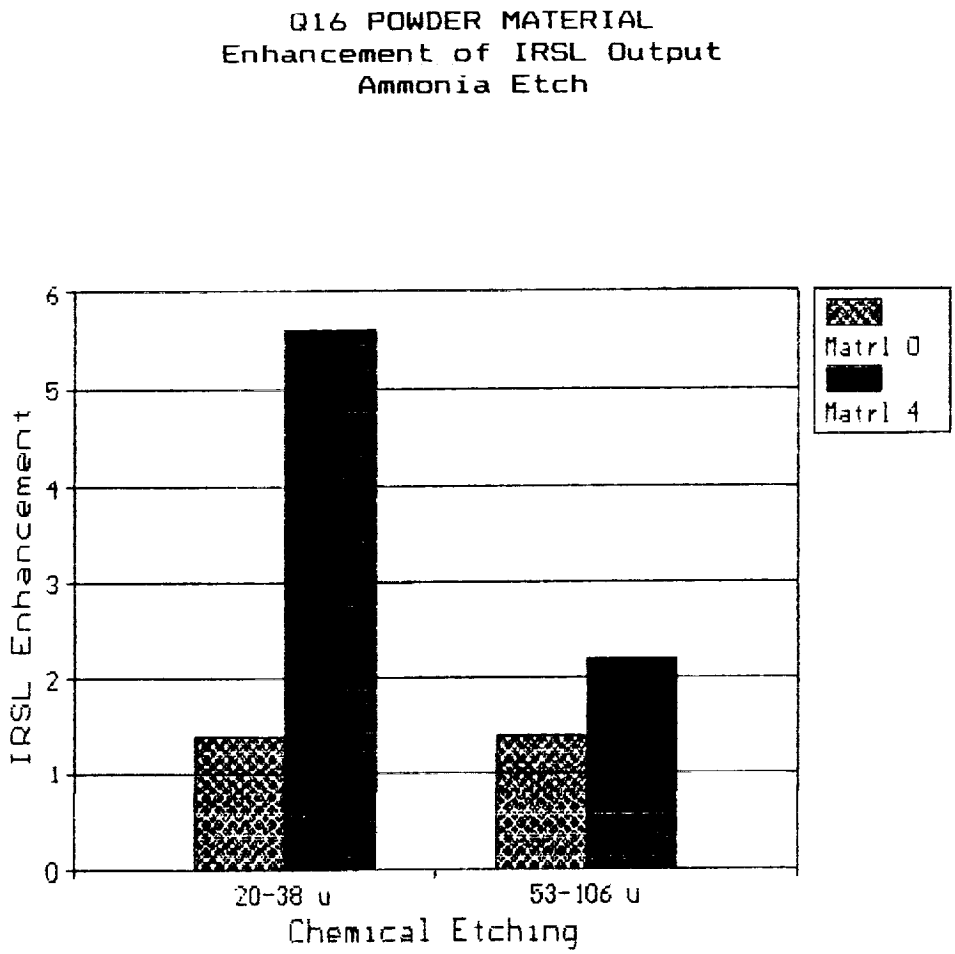

Figure 5. IRSL Enhancement of Ammonia Etched Q16 Powder as a function of particle size and material formulation.

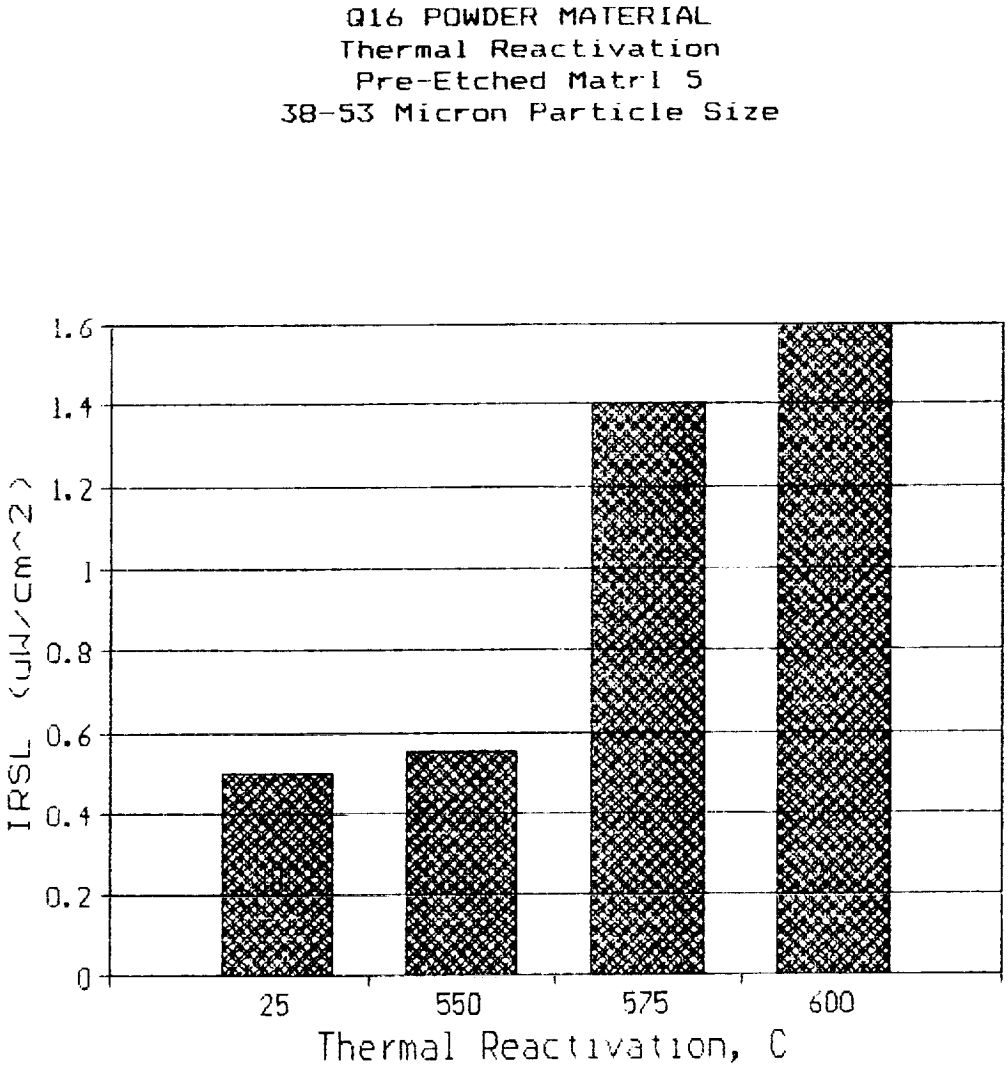

Figure 6. IRSL Output of Pre-etched Q-16 Powder vs. Reactivation Temperature.

temperature was increased to 600°C, the IRSL output was enhanced by a factor of 3.2. These results show that thermal reactivation at elevated temperatures does effectively anneal out effects of mechanical damage in the powder.

To test the overall powder process as a whole and determine how effective the powder process was in retaining the bulk ET properties, the most ineffective conditions of each of the process components were used and the final powders evaluated. This was accomplished by processing Matrl 0 and Matrl 4 ingots via Method 1, chemically etching using the ammonia etchant and thermally reactivating at 550°C. These results are shown in Figure 7 and Figure 8.

The IRSL output of Matrl 4 for 20-38 micron particle size distribution for each of the powder process components and the overall powder process are shown in Figure 7. As the contributions to the IRSL output are summed from the chemical etching and the thermal reactivation components an overall IRSL enhancement of over an order of magnitude (i.e. a factor of 12) was obtained as compared to the initial powder. In Figure 8, Matrl 0 and Matrl 4 are compared as a function of the IRSL output for each of the powder process components and the overall powder process are presented. For both Matrl 0 and Matrl 4 powders, dramatic improvements in IRSL output were obtained employing the modified powder process as compared to the initial powders. Additionally, these results show the IRSL output of the powder approaching the IRSL output of the bulk ingot, indicating that the ET properties of the powder material were effectively restored. In fact, the resulting IRSL output of Matrl 0 powder in Figure 8 was 95% of the IRSL output of the ingot.

Summary of ET Material/Powder Refinements

The ET bulk material optimization efforts produced substantial improvements in the material performance. The results showed a factor of 3 enhancement in the IR stimulated luminescence output and a 30% enhancement in the retention decay rate of our "Q-16" ET material. The improvements were a direct result of simplifying the material chemistry and variations in material content, form, and chemical compatibility.

The ET material permutations were both in material form and content from our standard oxide and sulfide rare earth dopants to the chloride version, along with the replacement of our more standard alkaline sulfate flux additive with an alkalai carbonate. The optimization variations that generated substantial material improvements employed low melting point chemical components that provide favorable thermodynamic properties for easing the crystallization process in the ET material.

To further optimize this ET storage material, further material variations are possible to provide yet more favorable thermodynamic properties to enhance the crystallization process. Alternate material forms such as other low-temperature alkalai carbonates and low-temperature rare earth dopants are currently being investigated in our on-going in-house material development efforts at Quantex. Alternate heating conditions to provide

Q16 POWDER MATERIAL
IR Stimulated Luminescence (IRSL)
20 - 38 Micron Particle Size
Matrl 4

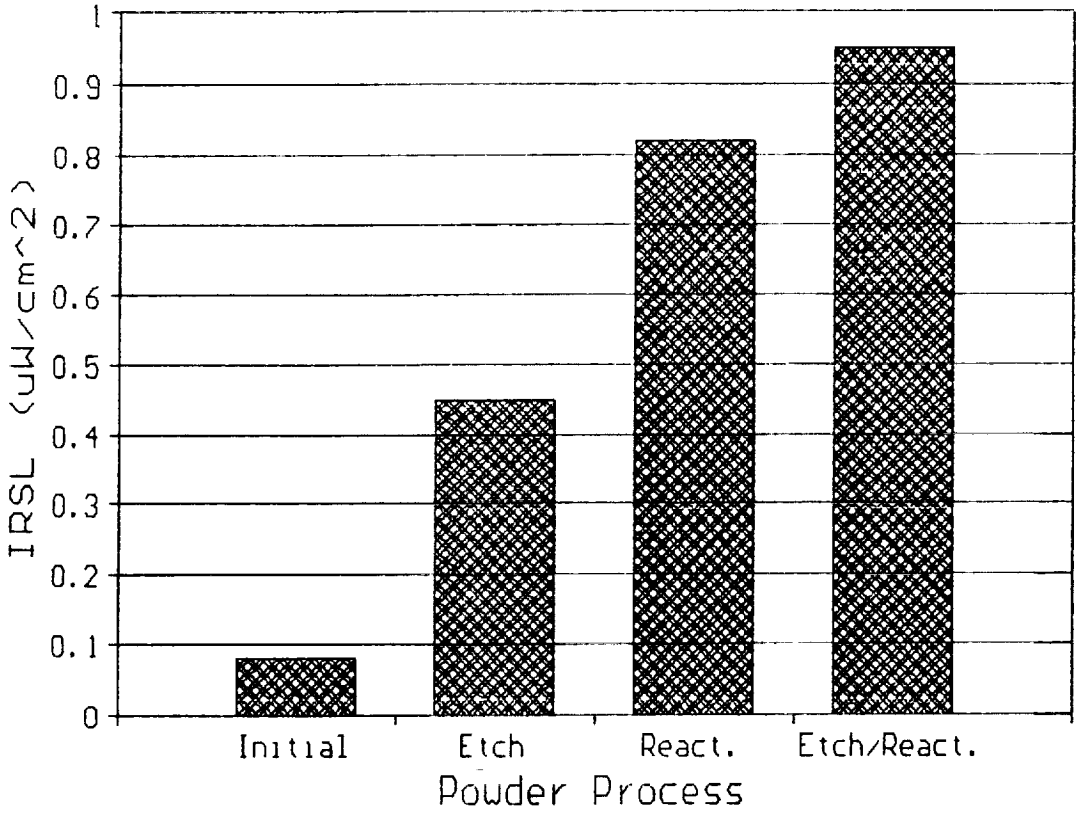

LEGEND

Initial	--	Initial Powder.
Etch	--	Powder after Chemical Etch.
React.	--	Powder after Thermal Reactivation.
Etch/React.	--	Powder after Chemical Etch and Thermal Reactivation.

Figure 7. IRSL Output for Various Powder Treatments.

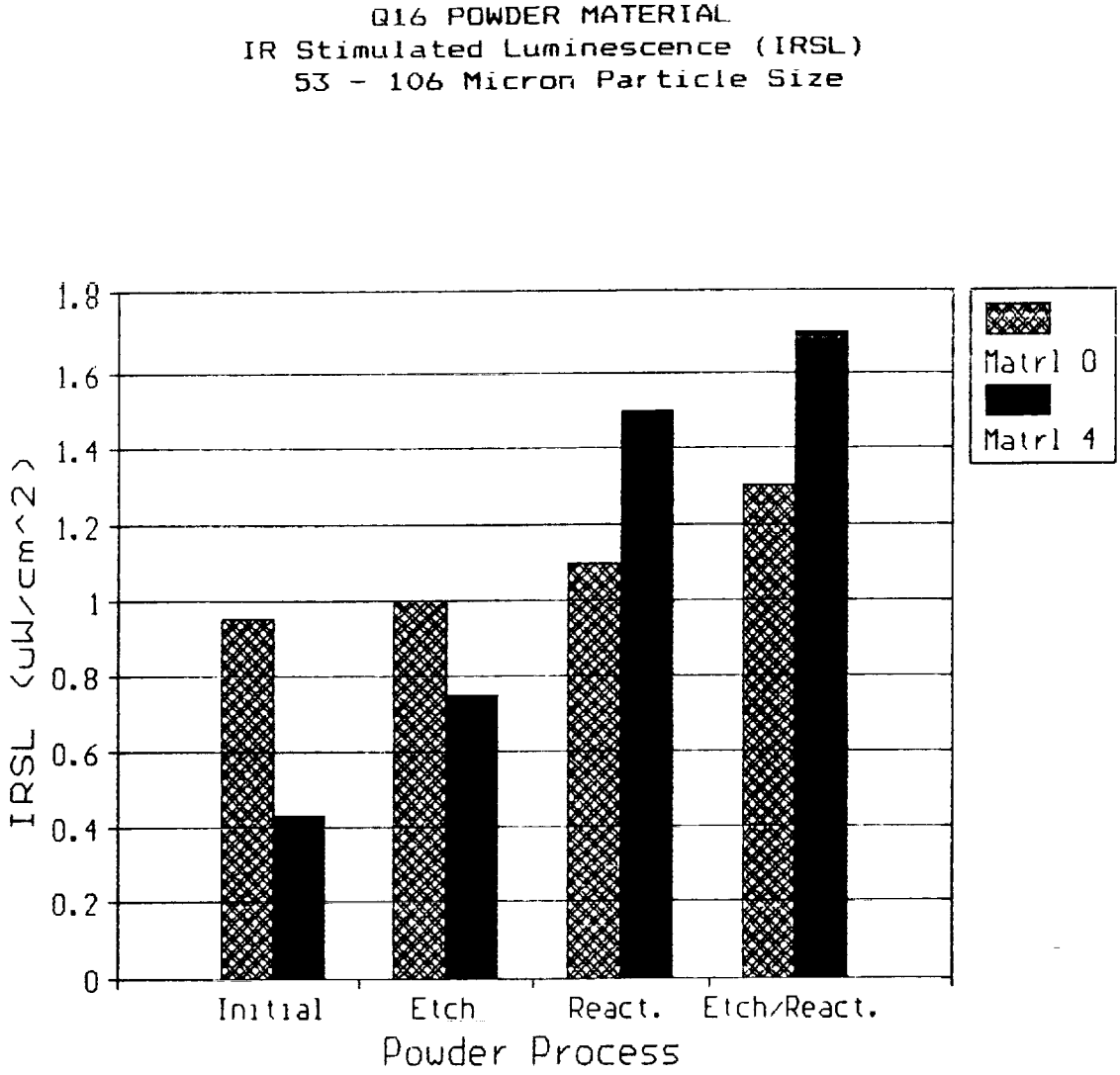

Figure 8. IRSL Output for Various Powder Treatments on Material Formulations 0 and 4.

additional favorable thermodynamic conditions to enhance the crystallization process are also being currently investigated. These material variations take the form of further simplifying the material chemistry, material content, chemical form and chemical compatibility.

The powder optimization effort during the contract term augmented an effective three-step powder process that converts bulk ET material into powder material for a large range of particle sizes. Each step of the powder process addressed the critical issues of minimizing and repairing surface and internal mechanical damage sustained during powdering. The development of each step of the powder process resulted in substantially improving the ET properties of the powder material. The evaluation of three powdering methods established an initial step to minimize the mechanical damage and improve the initial ground powder by a factor 3 in IRSL output. An improvement by a factor of 2 to 5 in the IRSL was achieved upon chemically treating the initial powder with ammonia-based etchants. Similarly, an improvement by a factor of 3 in the IRSL was achieved upon thermally reactivating the initial powder at an elevated temperature of 600°C. The total contribution of the steps in the powder process has resulted in an order of magnitude enhancement of the IRSL as compared to the initial status; 95% of the ET properties of ingot-form Quantex Q-16 Standard Material has been retained via this process.

To further improve the powder process and enhance the ET properties of the powder, a further development effort is required in establishing a more effective powdering method such as high velocity inert gas grinding and in establishing a more effective thermal reactivation stage such as roto-vac techniques to thermally reactivate the powder at higher temperatures with minimal agglomeration effects, i.e., to maintain separation of the powder particles buoyed in a neutral gas stream.

Device Fabrication

A number of detector plane fabrication techniques were investigated during the Phase II effort. The initial focus was on the fabrication of planes that would detect individual alpha particle events. A secondary consideration was to have planes available with a sufficient signal to noise ratio (SNR) so that the detection system could be evaluated for noise sources.

After detecting individual alpha particle events and reducing the detection system noise, efforts were then directed towards fabricating planes for the specific application in mind - i.e., the detection of cosmic ray particles. In this application, both thin detection layers and thin, low atomic number substrates are required since there should be minimal deviation of a particle from its path when passing through several detector planes.

In the following, the various methodologies for fabricating the detector planes are described. Included is a detailed description of the methods that were employed for fabricating thin phosphor layers on thin plastic films.

1. Thick ET powder layers on ceramic substrates

The primary method for obtaining thick film ET layers on ceramic substrates was to take powders having a particle size distribution of either 20-38 micrometers or under 20 micrometers, mix them thoroughly in alcohol, pour the resulting suspension into a vessel containing either an alumina or sapphire substrate, and then let the particles settle out onto the substrate. Next the alcohol was allowed to evaporate, the substrate was removed to a furnace and annealed at high temperatures (above 800°C). The flux remaining in the ET powder liquefies at this temperature and binds the powder together and to the substrate. In addition, the high temperature reactivates the electron trapping luminescence in the powder that had been damaged in the powdering operation. Samples having active areas of 2.5cm x 2.5cm, 5cm x 5cm and 10cm x 10cm were fabricated. Thicknesses ranged from 30 micrometers to 300 micrometers for the various samples made.

The samples fabricated as described above were primarily employed to verify simple alpha particle events, to check out the scanner detection system and to evaluate the ET materials. Much of the work performed involved the use of these detector planes. Such planes had limitations beyond their impracticality for the ultimate application. For example, they were subject to mechanical damage and environmental degradation. This resulted in spurious pulses when read out with an intense infrared laser beam and in reduced signal as the plane degraded. Also, the detector planes had fine infrared light absorbing particles incorporated in the phosphor layer that resulted in spurious signals. This indicated the need for employing purer materials as well as protecting the ET materials from mechanical damage and environmental degradation.

2. Vapor-deposited thin films on glass substrates

As the ET material and system evaluation proceeded, it became clear that there were two possible types of detector planes that could be fabricated to meet the requirements; namely, vapor deposited thin films on thin glass substrates or thin powder layers in an organic binder bonded to a thin plastic film. In this section, methods employed to deposit thin films are presented.

A principal issue in obtaining photonically active vapor-deposited films is to assure that all the target constituents end up on the substrate in approximately the proportions as in the target. With electron beam depositions, this will happen if the deposition rate is 15nm/s or greater. The resulting film is amorphous to microcrystalline, and requires a crystallization anneal at elevated temperatures to obtain full activation of the photonic properties. In the contract effort, solid pieces of SrS:Ce,Sm were electron beam deposited at high rates (15-20nm/s) and then subsequently annealed at 700°C to 850°C. Films were approximately 4 micrometers thick. Sapphire and quartz substrates were employed. At the beginning of the effort, films had no observable electron trapping properties, but as greater experience was gained, parameters for the anneal were found that resulted in photonically active films.

Adherence of the thin films was a problem, but a few 2.5cm x 2.5cm detector planes were fabricated with good adherence. However, experience with the deposition of other formulations of the ET materials indicated that a

substantial effort was required if films of sufficient thickness (20-50 micrometers), mechanical properties and performance were to be fabricated to meet the requirements of the contractual effort. Consequently, a decision was made to cease the thin-film vapor deposition efforts for this application, and concentrate of fabricating ET powder screens on plastic substrates.

3. Thin ET powder layers on thin plastic substrates

Work for the latter part of the effort was focused in the preparation of powder layers held together with low-temperature polymer binders. To repeat, this was motivated by:

a. The potential for employing thin substrates of low effective atomic number,

b. The higher sensitivity of the powders as compared to thin vapor-deposited films, even though some sensitivity is lost by having an organic binder,

and c. Only low temperature treatments consistent with polymer stability are required.

The detector plane fabrication efforts employed carefully activated ET powders of particle sizes ranging from a few to 38 microns, applied to acrylic, polyimide and polyester substrates. The application techniques of both screen printing and "doctor blading" were experimentally evaluated.

Acrylic substrates were coated with powder films employing Acryloid B 66 (Rohm & Haas) binders. The polyimide (Kapton) and polyester (Mylar) substrates (provided by L. Barbier of GSFC) were coated with powder films employing cyanoethyl starch (CNES) binders from Tel Systems and dimethyl formamide + cyclohexanone solvents.

Employing screen printing was less than satisfactory, because depositing the powder suspension through the screen mesh tended to produce non-uniform films on a microscopic scale. This would produce non-uniform ET performance from point to point for high-energy particle passage.

Consequently, we concentrated efforts on applying the powder/polymer suspension by the doctor blading technique, which simply trims a powder suspension slurry puddle to thickness by drawing a precise straight blade across it at a precise height. Adjustment of parameters such as viscosity and curing technique resulted in satisfactory films of some 75 microns thickness. The most successful films were those fabricated on clear polyester film substrates. Powder/polymer-binder films were successfully fabricated on all three substrate types, (except on some very thin metallized polyester films supplied by GSFC, which were wrinkled and difficult to keep flat enough for deposition control).

The best packing density was obtained with ET powder/binder films of 75 microns thickness on polyester substrates with a powder/binder volume ratio as high as 2:1. These employed ET powder of size distribution within 10 to 38 microns.

Task 2: Prototype Readout System

As outlined earlier in this report, an optical/electronic prototype readout system was needed to evaluate storage detector plane performance and to provide two-dimensional data on energetic particle impingement locations. The components of the prototype readout system were identified and ordered within two weeks of the contract start date. Delivery and assembly were completed by the 15th of July 1988, at which time experimentation began. The experimental apparatus as initially configured was as seen in Figure 9. A sample detector plane was mounted on the X-Y stage and stage motion was effected by an Aerotech Unidex 11 controller. Infrared light (1064nm) from an Amoco Laser diode-pumped YAG:Nd laser Model No. ALC-1064-50 was directed through lenses and mirrors and focused onto the sample through a 20X objective lens. Beam spot diameters under 20 micrometers could be attained by proper adjustment of the beam optics. A substantial portion of the luminescence produced by the ET plane was projected back through the objective lens, deflected by a beam-splitter, and detected by a Hamamatsu type R647 photomultiplier tube. The photomultiplier tube output was connected directly to a Tektronix model 468 digital storage oscilloscope's 1 MegOhm input terminal. The scanning table, optical system and detector were mounted within a light-tight enclosure on a vibration-isolated optical table.

Over the succeeding months, various changes were made to the readout system with the goal of providing a two-dimensional display of the readout. By the fourth quarter, a Keithly high-speed digitizer was installed and software for its operation was written. The system flexibility was checked out to determine how to best capture and display the data. A thermoelectric cooler was installed to further reduce photomultiplier noise.

In the fifth quarter, the thermoelectric cooler was installed and software was written that allowed for greater flexibility in the use of the Keithley digitizer. Experience with the digitizer led to a decision to replace it with a "photon counting" device to count each electron shower in the photomultiplier tube as a discrete pulse resulting from each photon received during readout. At first we employed a Stanford Research SR400 dual-channel gated photon counter, but finally we installed a Thorn-EMI C660 counter board. The Thorn-EMI board was installed into the data capture/imaging microcomputer and, as a result, can transfer data at much faster rates. This is advantageous because the high data rates allowed then minimize the "dead time" between count periods, and thereby missed counts while scanning.

We felt that photon counting would be a more appropriate method of data capture during readout scanning, due to the low photon fluxes involved from the small storage volumes produced on the detector planes by energetic particles. Photon counting methods allow the light impingement to be integrated over the entire count period, rather than sampled at a fixed rate as with the analog-input Kiethley digitizer. Also, the combination of cooling the photomultiplier tube and using the appropriate discriminator circuit allowed for very low noise measurements. We felt that the increase in the "active time" associated with the Thorn-EMI board would help minimize statistical uncertainties by increasing the total number of counts accumulated at each event site. Comparative measurements indicated that these assumptions were essentially correct. The signal to noise ration was increased by a factor of two.

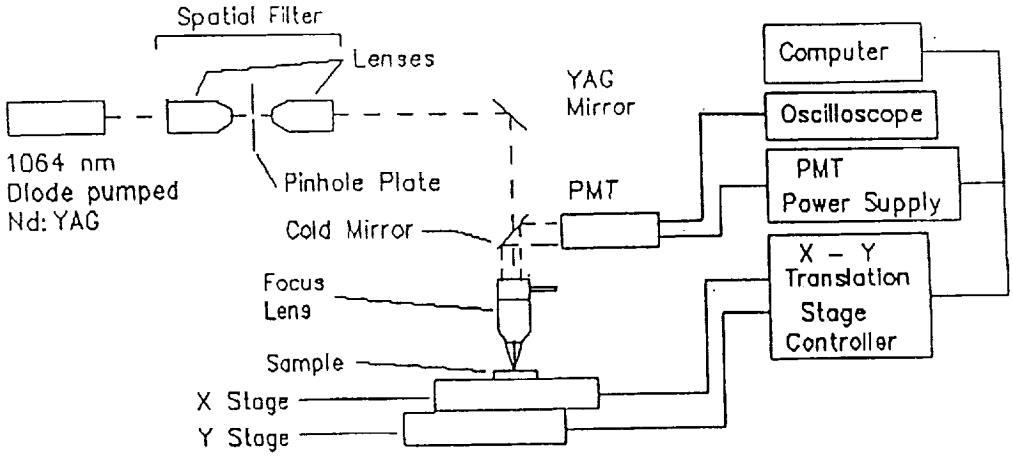

Figure 9. Readout scanner configuration.

Evaluations were also made to determine the optimal laser power (or optical power density) for the system in reading out ET detector planes. Results showed a peak signal to noise ratio at 2-3 mW total optical input power, as shown in Figure 10. This was roughly an order of magnitude less than we had previously employed. Optical neutral density filters were used in the YAG:Nd laser beam path to set the beam power.

Minor final changes in the optics were also made to improve system performance. A microscope objective with a 1.14 mm working distance was substituted for the original 0.40 mm working distance objective. This was done to increase the effective depth of field for both focussing the YAG:Nd laser beam as well as capture of the visible-wavelength emitted light. This objective has a numerical aperture of 0.7.

Several changes were also made to the synchronizing circuitry. Pulse widths and delay times were altered to better synchronize the count periods to the position of the translation stages during scanning.

Task 3: System Evaluation

As indicated above, a number of different detector planes were fabricated during the Phase II effort. At the beginning of the effort, the focus was to determine if single alpha particle events from a ^{210}Po source could be recorded and subsequently read out. In this, we were partially successful, but there was a considerable level of noise in the measurement system and the detector plane. Consequently, the distinction between real events and noise was difficult to make. Further, the detector planes were atmosphere sensitive, with the sensitivity to radiation decreasing with time. These initial results, however, provided a direction to the subsequent effort. This included improvements in the ET material, improvements in detector plane fabrication and reduction of noise levels in the measurement system.

Improvements in the ET material and detector screen fabrication are discussed in previous sections of this final report. In this section, improvements in the measurement system and measurement results will be presented.

After a few months effort, noise was considerably reduced. Proper grounding of system components and deep erasure of the detector planes allowed for the observation of a train of light output pulses on an oscilloscope that were due to alpha particle generated trapped electrons. This result is seen in Figure 11. Along with the alpha particle related pulses, some large spurious pulses were observed, most of which appeared to be associated with the detector planes. Efforts were directed towards understanding the origin of these pulses and their elimination. Their appearance was found to be related to the infrared beam intensity - i.e., the higher the beam density, the greater the number of pulses. At least two possible causes were determined. First, the presence of dust on the surface of the planes and small infrared absorbing particles (possibly carbon) within the phosphor layer were probable contributors, because the high light intensity was likely to heat the particles to incandescance. Second, it was found that mechanical damage to the phosphor produces light that results in trapped electrons as well as a light absorbing residue. In the first

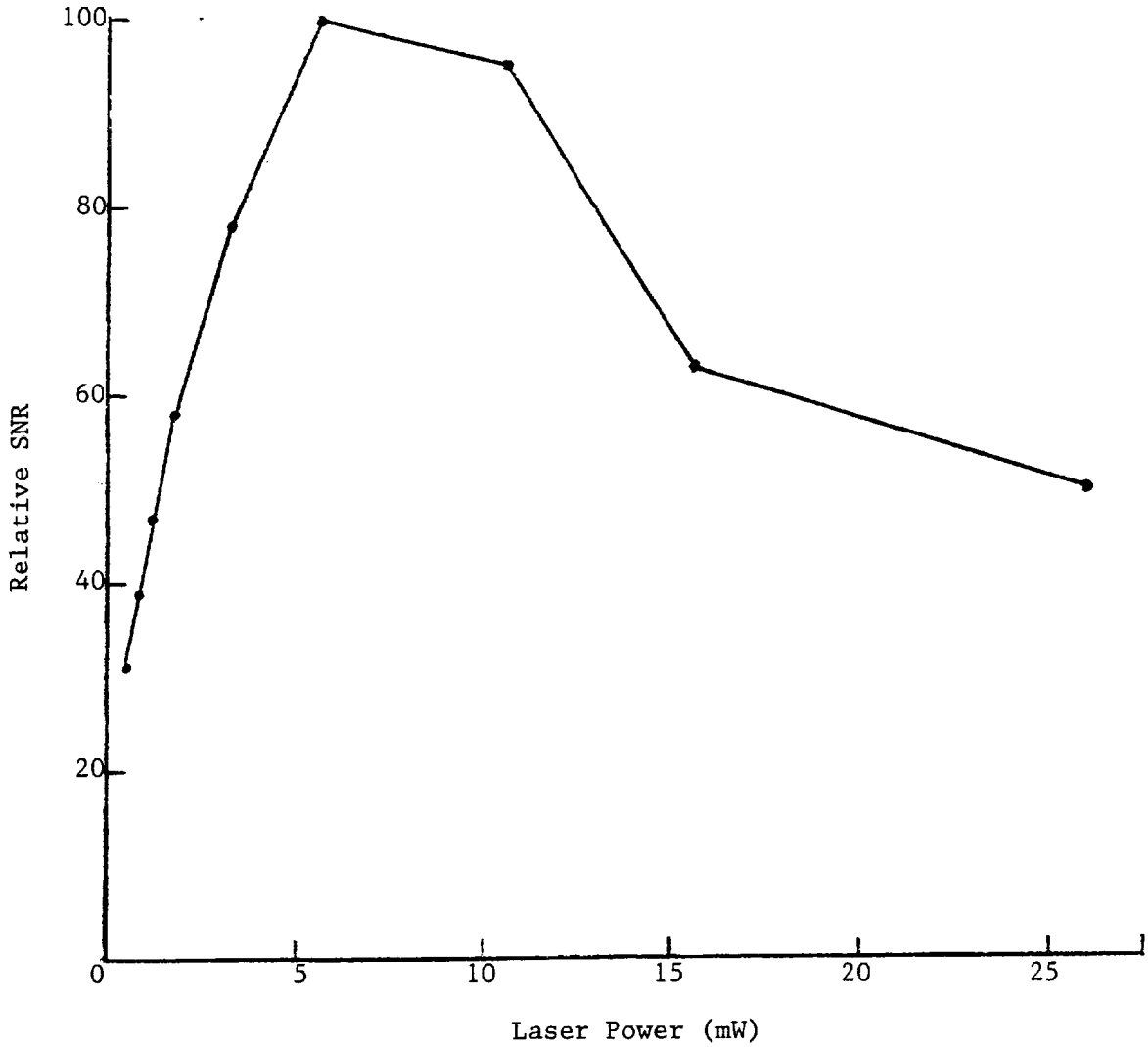

Figure 10. SNR dependence on incident near-IR laser power.

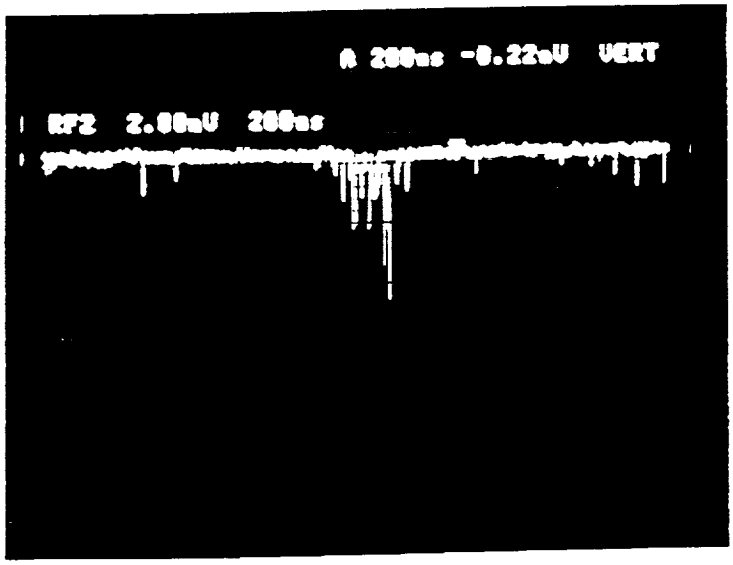

Figure 11. Oscilloscope trace of a train of pulses associated with individual alpha particle tracks.

instance, the trapped electrons would be removed after a single scan, whereas it is probable that the heating of the residue would produce bright light pulses with each scan. Since, in this stage of the contract effort, the phosphor layers were unprotected, mechanical damage from normal handling was likely to occur from time to time.

These results clearly indicated that the detector planes had to be fabricated differently and the infrared laser intensity at the detector plane had to be reduced. A number of detector planes were subsequently fabricated on sapphire substrates with particular attention being paid to high responsitivity and high ET powder particle density. After exposure to the alpha particle source, a pattern as shown in Figure 12 was obtained from the scan-out. Read-out laser intensity was reduced from the earlier measurements. The most important result was that the maximum number of photons detected in a given pixel was no greater than 25. The maximum number of noise counts was 5 per pixel.

As a consequence of these results, progress in powder preparations, and conversations with NASA-GSFC technical personnel, a decision was made to work towards a detector plane fabrication technique that involved the application of ET powders onto thin plastic substrates. Concurrent with this effort, a more detailed evaluation of the processes that result in a trapped electron population because of the passage of alpha particles was undertaken. The alpha-ray particle energy from the ^{210}Po source is approximately 5 MeV. This will result in approximately 4 x 10^5 electron-hole pairs being generated. The maximum electron energy expected is only a few thousands of electron-volts,and most electrons will have energies considerably less than 1 KeV. Consequently, the total volume that will be excited by the passage of an alpha particle will be small (on the order of 10^{-12} cm^3 or less). Further, the excitons that are created will have a short (less than 100 nm) path length, because the average separation distance of the rare earth dopants is considerably less than 100 nm. Therefore, it is estimated that there will only be 10^4 filled electron traps in the interaction volume after the passage of the alpha particle. (This is based on estimates of trapped electron populations in the bulk material from which the detector planes are made).

Taking into account the light that leaves the plane to pass through the collection optics to the photomultiplier tube, the maximum number of photons likely to be counted is in the range of 50 to 100 per alpha particle event. This number will be further reduced by any partial erasure of the trapped electron population by scattered infrared in advance of the scanning infrared beam focal spot. Also, if the light produced is shared between pixels, there will be an apparent reduction in the number of photon counts per alpha particle per pixel. Consequently, the observed number of photons per pixel per alpha particle event appears reasonable given the above comments.

This analysis suggests that it should be easier to detect very fast heavy particles since the interaction volume should be considerably larger that that of the relatively low energy alpha particles. The reason for the greater interaction volume is the production of delta rays that have sufficient energy to generate electron-hole pairs in a greater volume.

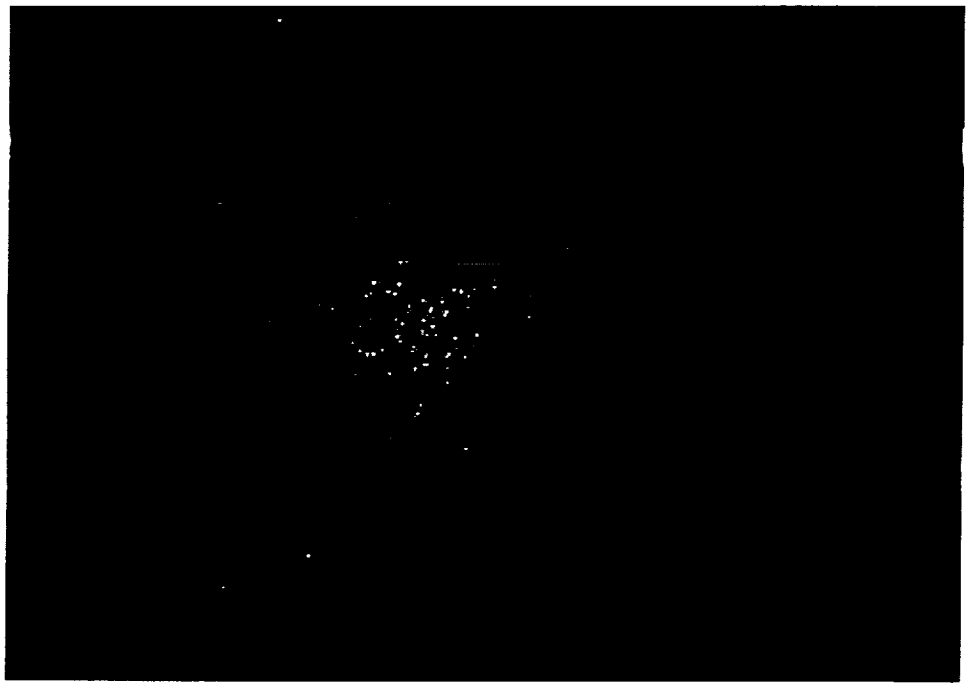

Figure 12. Two-dimensional image of alpha particle events recorded in an ET detector plane.

In the following, a table is presented that gives the calculated energy loss of selected nuclides in ET layers having different thicknesses[2].

Table 1. Energy Loss vs. Thickness

Primary Nuclide	Energy (GeV/nuclide)	Thickness (microns) 25	50	100	150
		Energy Loss (MeV)			
Hydrogen	3		0.015	0.030	0.046
Lithium	5	0.076	0.145	0.290	0.436
	15	0.083	0.167	0.330	0.502
Oxygen	5		1.033	2.070	3.100
	15		1.191	2.380	3.570
Iron (^{55}Fe)	15	6.286	12.572		
(^{56}Fe)	15	6.286	12.572		

Most of the energy is lost in the production of delta rays, and, for the heaviest nuclides, quite high energy delta rays are produced. This is seen where the following formula relating the number of delta rays produced with energies between E_0 and E_{max} per g/cm^2 of material is applied:

$$N(Z, E>E_0) = \frac{\alpha Z^2}{\beta^2}\left[\frac{1}{E_0} - \frac{1}{E_{max}}\right] - \frac{\alpha Z^2}{E_{max}} \ln[E_{max}/E_0]$$

where $$\alpha = 1.536 \frac{Z_{target}}{A_{target}} \quad \text{(in MeV/gm/cm}^2\text{)}$$

Z = atomic number of the high energy particle

Z_{target} = atomic number of the target

A_{target} = atomic weight of the target

$$\beta^2 = \frac{v^2}{c^2} = 1 - \frac{1}{\gamma^2}$$ where γ is the Lorentz factor

and $E_{max} = 2m_e c^2(\gamma^2 - 1)$, where m_e is the electron rest mass.

Production of high energy delta rays is favored by high-energy, heavy particles. However, there is a spectrum of delta ray energies, with a greater number produced at lower energies. Qualitatively, it appears that the excitation volume will be considerably greater than that for low energy alpha particles (possibly two orders of magnitude greater), and, as a consequence, the limiting factors on the detection of the high energy particles will be the energy lost in the ET material, the trapping efficiency, and the optical efficiency of the detection system.

Table 1 gives the energy loss. The likely electron-hole pair generation for the energy loss in a 50 micrometer layer of ET material is seen in Table 2 below.

Table 2. Electron-Hole Pair Generation For Various Nuclides

Nuclide	Energy/nuclide (GeV/nuclide)	Energy loss (MeV)	Projected number of electron-hole pairs generated
Hydrogen	3	0.015	1×10^3
Lithium	5	0.145	1×10^4
	15	0.167	1×10^4
Oxygen	5	1.033	8×10^4
	15	1.191	9×10^4
Iron (^{55}Fe)	15	12.572	1×10^6
(^{56}Fe)	15	12.572	1×10^6

A fraction of the electron-hole pairs generated will result in trapped electrons. At the present stage of development of the ET materials, the best trap-filling efficiency is estimated to be 10%. It may be possible to increase this further with additional effort.

Another factor is the optical efficiency of the read-out system. Taking into account the photomultiplier tube's photocathode efficiency, the light capture efficiency of the optical system and the percentage of light generated that exits one side of the ET layer, only about 1% of the light that is generated is being detected. By careful design of the optical system and selecting a high efficiency photomultiplier tube, it may be possible to increase the overall optical efficiency up to 8-10%.

At present, it appears that it may be possible to detect heavy particles with atomic numbers greater than 8 (oxygen) with an acceptable signal to noise ratio. With improvements in the material, collection optics and detector, lithium may be detectable.

The above discussion has dealt with a 50 micrometer thick ET layer. Use of such a layer will result in the ability to detect events with a resolution of approximately 20 micrometers if 1) the diameter of the scanning beam is kept less than 20 micrometers, 2) the particle size of the ET phosphor is on the order of a few micrometers, and 3) the scan is

performed rapidly. The signal to noise ratio obtained from a plane of this thickness will be dependent on the scanning strategy. Both the scan speed and the step-over distance will determine the optimum laser power required for the best signal to noise ratio. Further experiments are necessary to determine the best scanning parameters. Specifically, the planes need to be exposed to heavy charged particles and then read out. These planes will need good retention of the trapped electron population; particularly if they are to be shipped back and forth from accelerator facilities. Hence our work on this aspect of the ET material during the term of the Phase II contract. Good retention of electrons in traps (>80% over 24 hours) has been demonstrated for ET powder particles of 20 microns in size. This needs to be extended to powder particles of less than 10 micron size.

A 50 micrometer ET layer on a 50 micrometer plastic substrate will not result in any substantial deviation of the incident high energy particle. Consequently, it should be possible to track a given particle through several detector planes.

In summary, the detection of cosmic rays appears to be possible with detector planes constructed of ET layers bonded to thin polymer substrates. Further improvement of the ET materials and upgrading of the detector system are required if light nuclei such as lithium are to be detected.

Task 4: Preparations for Phase III

Since the beginning of this effort, it has been realized that the detector plane configuration required for successful completion of this project may not have substantial commercial application. However, it was strongly felt that many of the processes developed could have a major impact on other types of detector planes that would have commercial viability.

This has indeed been the case, as Quantex's marketing and sales staff have generated considerable interest in radiation sensitive detector planes for industrial/aerospace/biomedical applications. In particular, high resolution wide dynamic range detector planes such as are required for this program could have immediate application in the area of X-ray crystallography of biological, organic and inorganic crystals. Quantex is presently exploring this area of possible commercial application further.

At the end of this Phase II effort, a path for attaining the capability for detecting cosmic ray particles has been established. Additional work is required to fully implement detector plane fabrication techniques for space application. As a consequence, it is premature to generate engineering documentation on detector plane fabrication and the associated readout instrumentation for a Phase III partner.

Additional efforts to refine our capabilities for detecting cosmic ray particles are likely to generate even further commercial applications, because the NASA requirement demands very high performance detector planes as well as high performance readout systems. Specifically, high performance ET storage materials of yet finer particle sizes, the ability to fabricate large area planes, and the construction and exercise of a high sensitivity detection system are likely results of any further efforts.

Task 5: Reports

The specified Quarterly Reports and this Final Report were generated and submitted to NASA GSFC.

CONCLUSIONS:

This SBIR Phase II effort has defined the requirements for a detector plane that will record the passage of a spectrum of cosmic ray particles, and such planes have been fabricated. This work has involved the development of techniques for producing high efficiency electron trapping powders as well as for fabricating detector planes.

Although no substantial commercial use for a cosmic ray detector is foreseen, these same detector planes are likely to have a myriad of uses in the commercial marketplace, since they are sensitive to all types of ionizing radiation. The extended dynamic range of this system vs. photographic film would offer definite advantages in such areas and the direct data capture would facilitate image analysis. Among the readily identifiable uses are radiation beam pattern profiling, autoradiography (e.g., isotope tagged biological materials), industrial radiography, crystallography, and medical radiography.

Quantex is pursuing a number of these applications, both with internal funds and with the support of commercial partners. Consequently, the work performed in this Phase II effort has been very successful with regards to its particular objectives and to the overall objectives of the SBIR program.

For the various likely commercial applications or larger volume applications to NASA projects, it would be advisable to complete engineering implementation of powder manufacturing systems such as inert-gas jet milling and cyclone particle size separation for production quantities. Such equipment was beyond the financial scope of the Phase II work, but is readily available.

It would be highly worthwhile to proceed on to NASA tests with accelerator-produced high-energy nuclide mapping and then to balloon-flight sampling of cosmic-ray relativistic nuclide recording trials. This would provide a final demonstration of the capabilities of the ET detector plane system and data for subsequent NASA application in orbital experiments. Such planes and readout systems should be very useful for NASA in obtaining data at orbiting or space-vehicle locations on the characteristics of relativistic nuclides, as originally desired at the inception of this project. In particular, the advances made near the end of the Phase II work in very lightweight detector planes should allow high-resolution position determination with little deflection by the detecting planes.

NEW TECHNOLOGY:

During the course of this effort we have mainly applied pre-existing (proprietary or patented) Quantex ET materials technology or techniques "known in the art" in phosphor technology, and off-the-shelf hardware, but have applied them to the specific needs of thin, lightweight planes for high-energy nuclear particle passage recording and a prototype readout system for them.

Consequently, we do not feel that there are any reportable items of New Technology that would pass U.S. Patent Office examination as "new art" for intellectual property.

BIBLIOGRAPHY:

1. Y. Kaneko and T. Koda, Journal of Crystal Growth, 86, p.72, (1988).

2. L. Barbier, NASA/GSFC, private communication.

NASA National Aeronautics and Space Administration

Report Documentation Page

1. Report No.	2. Government Accession No.	3. Recipient's Catalog No.

4. Title and Subtitle
Large Area Nuclear Particle Detectors Using ET Materials - Phase II

5. Report Date
May 1990

6. Performing Organization Code

7. Author(s)
C. Wrigley, G. Storti, L. Walter and S. Mathews

8. Performing Organization Report No.
LAPD-FINAL

10. Work Unit No.

9. Performing Organization Name and Address
Quantex Corporation
2 Research Court
Rockville, Maryland 20850

11. Contract or Grant No.
NAS5-30310

13. Type of Report and Period Covered
Final
5/9/88 - 5/9/90

12. Sponsoring Agency Name and Address
NASA/Goddard Space Flight Center
Greenbelt, Maryland 20771
Jonathon Ormes

14. Sponsoring Agency Code

15. Supplementary Notes

16. Abstract

This report presents work done under a Phase II SBIR contract for demonstrating large area detector planes utilizing Quantex electron trapping (ET™) materials as a film medium for storing high-energy nuclide impingement information. The detector planes utilize energy dissipated by passage of the high-energy nuclides to produce localized populations of electrons stored in traps. Readout of the localized trapped electron populations is effected by scanning the ET plane with near-infrared, which frees the trapped electrons and results in optical emission at visible wavelengths. The effort involved both optimizing fabrication technology for the detector planes and developing a readout system capable of high spatial resolution for displaying the recorded nuclide passage tracks.

17. Key Words (Suggested by Author(s))	18. Distribution Statement
Particle Detectors, ET Storage, Cosmic Rays, Electron Trapping	See SBIR Right Notice (June 1987)

19. Security Classif. (of this report)	20. Security Classif. (of this page)	21. No. of pages	22. Price
Unclassified	Unclassified	32	

NASA FORM 1625 OCT 86